Neuron, Vol. 42, 993–1001, June 24, 2004, Copyright ©2004 by Cell Press

Parietal Area VIP Neuronal Responses to Heading Stimuli Are Encoded in Head-Centered Coordinates

Tao Zhang,[1] Hilary W. Heuer,[1] and Kenneth H. Britten[1,2,*]
[1]Center for Neuroscience
[2]Section of Neurobiology, Physiology, and Behavior
University of California, Davis
Davis, California 95616

Summary

The ventral intraparietal area (VIP) is a multimodal parietal area, where visual responses are brisk, directional, and typically selective for complex optic flow patterns. VIP thus could provide signals useful for visual estimation of heading (self-motion direction). A central problem in heading estimation is how observers compensate for eye velocity, which distorts the retinal motion cues upon which perception depends. To find out if VIP could be useful for heading, we measured its responses to simulated trajectories, both with and without eye movements. Our results showed that most VIP neurons very strongly signal heading direction. Furthermore, the tuning of most VIP neurons was remarkably stable in the presence of eye movements. This stability was such that the population of VIP neurons represented heading very nearly in head-centered coordinates. This makes VIP the most robust source of such signals yet described, with properties ideal for supporting perception.

Introduction

When we move through the environment, the pattern of retinal image motion provides a rich source of information concerning our trajectory, or heading (Gibson, 1950). Human observers and nonhuman primates are very accurate at the task of recovering heading from such optic flow cues, with thresholds near a degree of heading angle under optimal conditions (Warren et al., 1988; Crowell and Banks, 1993; Britten and Van Wezel, 2002). Under natural conditions, we estimate our heading while the eyes are in nearly constant motion; this confounds the retinal optic flow field. When tested in the laboratory, subjects are remarkably good at compensating for smooth pursuit eye movements, and accuracy is little affected (Warren and Hannon, 1990; Banks et al., 1996; Royden et al., 1992, 1994). However, the neural mechanisms underlying the perception of heading and the compensation for eye movements remain largely unknown.

Most studies of neural signals representing optic flow have focused on the medial superior temporal area (MST; Saito et al., 1986; Tanaka et al., 1989; Duffy and Wurtz, 1991a, 1991b, 1995; Graziano et al., 1994; Bradley et al., 1996; Page and Duffy, 1999; Upadhyay et al., 2000; Shenoy et al., 2002; for review, see Andersen et al., 2000). However, MST is only one of several extrastriate and posterior parietal areas that potentially could inform heading judgments. These areas include the ventral intraparietal area (VIP), area 7a, and the superior temporal polysensory area (STP). These areas have not been well studied, but VIP in particular is a promising candidate due to its neuronal response properties. VIP receives visual input from many of the same areas as MST (Blatt et al., 1990; Maunsell and Van Essen, 1983; Lewis and Van Essen, 2000). Directional neurons are common in VIP (Colby et al., 1993; Schaafsma and Duysens, 1996; Bremmer et al., 2002a), and these neurons appear to be involved in motion detection tasks (Cook and Maunsell, 2002). Moreover, cells in VIP respond selectively to optic flow patterns such as expansion (Schaafsma and Duysens, 1996). The multimodal properties of VIP—it contains somatosensory and auditory responses in addition to visual motion—might make a structure useful in guidance of movements in near, extrapersonal space (Duhamel et al., 1998; Bremmer et al., 2002b), while recent microstimulation work suggests that it might play a role in defensive movements (Cooke et al., 2003). One property in particular, however, stands out with regard to a potential role in navigation. Many receptive fields (RFs) in VIP are not specified in the normal retinal coordinate frame, but instead appear to be fixed in space, despite changes in gaze (Duhamel et al., 1997). This property of compensation for current gaze direction implies that VIP has access to signals of eye direction or eye movements, presumably of extraretinal origin. Such signals have been strongly implicated in the compensation of heading perception for eye velocity (Warren and Hannon, 1990; Banks et al., 1996). Therefore, we hypothesized that VIP would contain an accurate representation of heading, and furthermore that this representation would be well compensated for ongoing eye movements. Our results support both of these predictions. Additionally, from our results, it appears that pursuit compensation is more complete in area VIP than was seen in the related experiments of Andersen and colleagues in MST (Bradley et al., 1996; Shenoy et al., 2002). Some of these results have previously appeared in a published abstract (H.W. Heuer et al., 2002, Soc. Neurosci., abstract).

Results

This study addressed two principal questions about heading representation in VIP. First, how well tuned are the neurons to heading? Second, how is this tuning affected by smooth pursuit eye movements? We studied the responses of 87 randomly selected neurons in VIP (28 from monkey C and 59 from monkey F). The sole inclusion criterion was that neurons be visually responsive; only a small minority of neurons were discarded for this reason. All of the included neurons were directional, all responded to large random-dot patterns, and all showed some degree of selectivity for heading.

*Correspondence: khbritten@ucdavis.edu

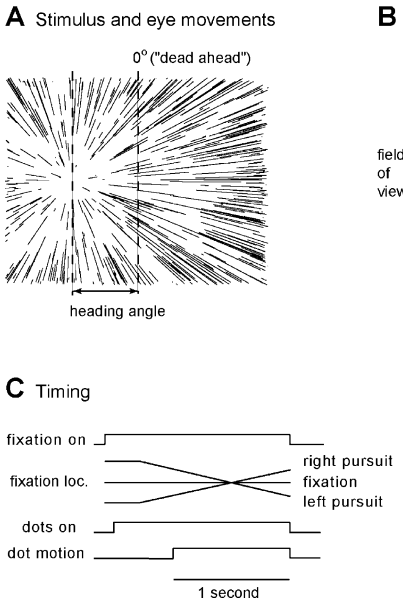

Figure 1. Stimuli and Task Timing

The heading stimuli we used are simulations of self-movement toward a 3-dimensional cube of dots.

(A) Observer view of an example stimulus. The center of this radial pattern indicates the heading. Heading angle is defined as the angle between dead ahead and the center of expansion.

(B) Top view of the simulated geometry of the task. The arrow shows the trajectory with respect to the simulated 3D dot field; its length is approximately to scale for the speed of the simulated trajectory. The vertical dashed line depicts dead ahead, or egocentric zero.

(C) Timing of events in single trials.

Single Cells in VIP Are Well Tuned for Heading

We measured VIP neuronal responses to stimuli simulating a range of horizontal heading angles, which varied from −30° (left) to 30° (right), at 5° intervals. Figure 1 illustrates the stimuli that were used for these measurements. On any trial, a dot pattern simulating a linear trajectory along a single heading angle was presented for 1 s, and responses were measured for the entire 1 s trajectory. Figure 2 illustrates three typical cells' tuning. The cells in Figures 2A and 2C show sigmoid tuning, monotonically changing through the range that we measured. On the other hand, the cell in Figure 2B was band-pass tuned for near-zero headings. We observed these three types of tuning (left-preferring, band-pass, and right-preferring) with nearly equal frequency in our sample of 87 cells.

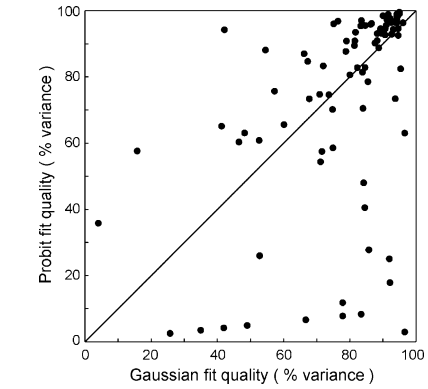

Figure 3. Analysis of Tuning Function Shape

We fit each cell's responses to both probit and Gaussian functions, then evaluated the quality of each fit by calculating proportion of variance (% variance explained = 100 × (1 − [variance (model − data)/variance (data)])). Data from one cell (1/88, 1.1%) were discarded due to very poor fits to both functions. For about 2/3 (59/87, 67.8%) of the cells, a probit function describes the tuning better than a Gaussian function. For the other 1/3 (28/87, 32.2%) of the cells, a Gaussian function captures the data better than a probit function.

Because of the diversity of tuning, no single function would describe all cells. We found that all cells in our sample, though, could be well described by either a sigmoid (probit) or Gaussian function. In order to accurately estimate parameters describing each cell, we needed first to find the appropriate function for each cell by comparing the goodness of fit of each type (probit or Gaussian). For each cell, we measured the percentage of variance explained by each (Figure 3). For a majority of cells, both functions captured the data well (points in upper right corner). This is unsurprising, as the flanks of a Gaussian curve are also sigmoidal in shape. These cells, then, have tuning that is dominantly sigmoidal in shape, and for these, the probit function provided the better account of their tuning (59/87; 68%). However, other cells clearly were much better described by the Gaussian function (points below the diagonal; 28/87, or 32%). These cells show genuine band-pass tuning.

It remains possible that the apparently sigmoid tuning of the majority of our cells is due to the limited range of heading angles that our hardware was capable of testing. Perhaps if we had tested to greater angles, these cells would have decreased their firing, resulting in band-pass cells tuned for far headings. Two analyses argue against this possibility. First, we analyzed the re-

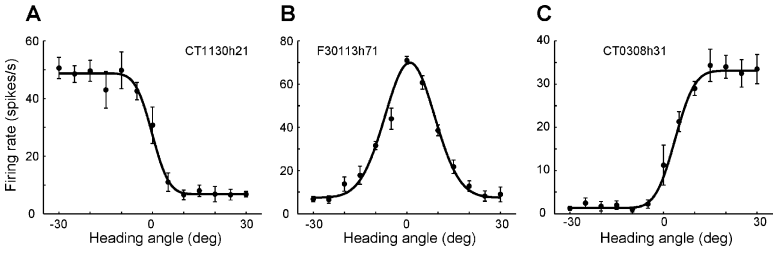

Figure 2. Three Typical Example VIP Neurons

(A) and (C) show the responses of two typical cells with open-ended tuning functions. Such cells were well described by probit functions (smooth curves). The cell in (A) has a mean of −0.1°, a bandwidth of 2.7°, and an amplitude of 42 spikes/s. Cell CT0308h31 in (C) has a mean of 3.7°, the bandwidth is 3.2°, and the amplitude is about 32 spikes/s. (B) shows a cell typical of the minority with bandpass tuning for heading; these can be well fitted by Gaussian function. This cell has a mean of 1.0°, a bandwidth of 4.7°, and an amplitude of 63 spikes/s.

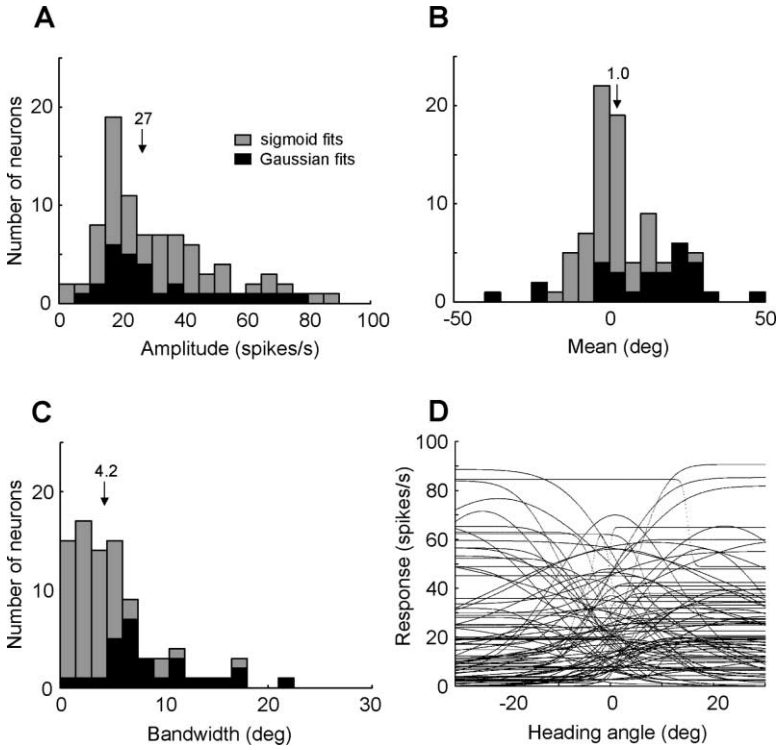

Figure 4. Sample Distributions of Tuning Parameters

Gray bars represent the sigmoidally tuned cells (probit fit superior), and black bars represent the bandpass tuned cells (Gaussian better).

(A) Amplitudes of tuning were very similar for both groups (medians were 26 spikes/s and 27 spikes/s for sigmoid and band-pass cells, respectively).

(B) Means were somewhat different for the two groups of cells, with the sigmoidally tuned cells having more central means. This difference is statistically significant by a t test (medians of -0.3° and 16.0°; $t = 3.80$, $p < 0.05$).

(C) The bandwidth of sigmoid cells (median = 3.0°) is significantly smaller than the bandwidth of band-pass cells (median = 7.3°; $t = 6.37$, $p < 0.05$).

(D) Composite plot of all tuning functions in our sample.

siduals from the probit fits. If these were band-pass cells, with peaks near the end of the range of headings tested, then the residuals would trend negatively near the end of the range. No such trend was evident in the residuals (data not shown). Second, the majority of sigmoid-tuned cells had both near-zero centers of tuning and narrow bandwidths (see below). The sigmoid function we used (probit) provided a good account of the data (Figure 4) despite being forced to be flat for a large range of the data, usually approximately 20°. Thus, for the tuning to be band-pass and for this kind of function to provide such a good account of the data, the data would have to remain near maximal for a long distance from the peak, despite having a steep flank; this seems unlikely to us. Despite these arguments, however, we remain agnostic as to whether the apparent dichotomy represents truly distinct categories or a continuum of properties. We are confident in either case that we have accurately described the cells in our sample, allowing us to quantify the heading information they represent.

The tuning characteristics of our neurons suggest that they are well suited to encode near-frontal headings very accurately. We analyzed the distributions of amplitude, mean, and bandwidth parameters from the best-fit functions (Figure 4). In each panel, the filled black bars denote band-pass cells and the gray bars show the sigmoid-tuned cells. First, it is evident that most cells showed considerable dynamic range in their responses related to heading. The average amplitude of nearly 30 spikes/s and the fact that many cells showed even higher tuning amplitudes indicates very good signal quality in VIP. Amplitudes were comparable between sigmoid-tuned and band-pass cells (Figure 4A). The distribution of center points of tunings, however, was far from uniform (Figure 4B). The sigmoid-tuned cells had a strong tendency to center near zero headings (dead ahead); the distribution was not significantly different from zero (t test, $p > 0.05$). On the other hand, for reasons that are unclear, the band-pass cells tended to have means to the right of zero, and their midpoints were more widely distributed. This distribution is significantly shifted to the right of zero (t test, $p < 0.05$).

Band-pass cells were apparently more broadly tuned than were sigmoid-tuned cells (Figure 4C). The mean bandwidth (defined in Experimental Procedures) for band-pass cells was 7.3°, compared with only 3.0° for the sigmoid-tuned cells, and this difference was statistically significant (t test, $p < 0.05$).

Our cells tended to be tuned near dead ahead and tended to have fairly narrow bandwidths, suggesting that the population would have more information available in near-frontal headings. This impression is supported by the composite tuning function shown in Figure 4D. In this panel, all the tuning functions are shown together. While the diversity of tuning is apparent, two features are evident. First, it is clear that there are considerably more oblique lines (inflections of sigmoidally tuned cells, flanks of band-pass-tuned cells) in the central 15° of heading. No constraint of our methodology could produce this feature; it reveals where the firing rates in VIP are changing most rapidly. The other evident feature is related—near the ends of the axis, most tuning functions are horizontal and parallel. This figure compactly demonstrates that the population carries more sensitive information about heading changes for central headings.

Influence of Pursuit on Single-Cell Heading Responses

Normally, we do not keep our eyes still when we move through the environment. During self-motion, the retinal

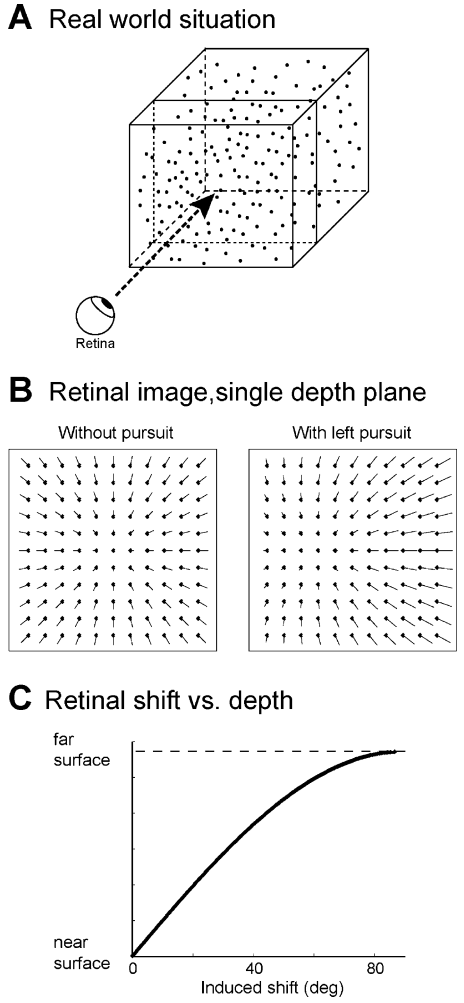

Figure 5. Effects of Gaze Rotation

(A) The geometrical configuration that our stimuli simulate, consisting of a linear observer trajectory toward a cloud of points.

In (B), we show the retinal flow fields (regularized for illustration purposes) at the single depth plane depicted in (A). In the right panel, one can see the horizontal shift of the flow field caused by left pursuit at 10°/s. If this depth plane were varied in depth, the amount of shift would systematically change in the manner depicted in (C), where the horizontal shift increases with increasing relative depth. See text for additional details.

image can be badly distorted by eye movements. Psychophysical experiments in both humans and monkeys show that perception can largely discount the effects of eye movements. To inquire whether VIP participates in this compensation process, we measured heading tuning in the presence of horizontal eye movements of 10°/s in both directions. This magnitude of eye rotation will cause large changes in the apparent (retinal) flow field, schematically illustrated in Figure 5. In Figure 5A, we show the familiar situation without pursuit. Image points directly ahead of the animal have no velocity; this produces the focus of expansion, which is the same for all depths. At any single depth plane (such as the one illustrated in 5A), the addition of the pursuit vector field causes a shift of the focus of expansion in the direction of pursuit, as shown in the right panel of Figure 5B. However, the amount that this focus shifts depends on the depth of the image plane. This is because the pursuit-induced retinal velocity is independent of depth, while the retinal velocities resulting from self-motion decrease with increasing depth. Thus, at larger distances, the pursuit velocities have a larger relative effect and the shift of the focus of expansion is greater. This is illustrated in Figure 5C, which shows the dependence of the retinal shift on the relative depth for the conditions of our experiment. These range from zero for the nearest dots and rise to approximately 80° (well off-screen) for the farthest dots. The average shift, therefore, is approximately 40°. The exact value would depend on the manner in which VIP cells average multiple velocities, which is unknown. This is the amount that one might expect the tuning functions to shift, if VIP were representing heading in retinal coordinates, and this is not what we observe.

VIP cells' tuning functions were remarkably little affected by pursuit (Figure 6). Three example cells are shown, and all show very good stability under pursuit. The solid curve shows the tuning with the eyes stationary; the broken curves show the tuning measured during left and right pursuit. It is important to realize that the tuning functions are plotted in screen rather than retinal coordinates. Therefore, curves that superimpose demonstrate tuning that is invariant under pursuit or, equivalently, encode heading in head-centered coordinates. The stability of these functions demonstrates that inputs that stimulate the retina very differently produce tuning that remains essentially fixed with respect to the head. Because the heads of our monkeys were fixed in the chair, it is of course impossible for us to distinguish whether the representation is closer to head-centered, body-centered, or exocentric ("world") coordinates. However, we can be quite confident that the representation is not in retinal coordinates.

The population of VIP cells, on average, appears to also contain a fairly stable representation of heading under pursuit. To characterize our sample of cells, we used the parameters of the best-fit tuning functions, and asked how these parameters were affected by pursuit. First, we considered the central tendency of the cells' tuning, captured by the mean parameter. Differences in this parameter resulting from pursuit are shown in Figure 7A. Shifts to the left (in screen or head coordinates) are indicated by negative values and rightward shifts by positive values. For both directions of pursuit, there was a slight shift opposite the direction of pursuit. From Figure 5, it was apparent that the center of expansion shifted in the direction of pursuit, so the average shift we see reflects a slight overcompensation for the retinal effects of pursuit. This result stands in contrast to the observations of Andersen and colleagues on MST (Bradley et al., 1996; Shenoy et al., 2002), which indicated that neurons in MST undercompensated for pursuit, on average. Of the two directions of pursuit, the sample means were significantly shifted only for left pursuit (t test, $p < 0.05$). Also, band-pass and sigmoidally tuned cells were similarly stable under pursuit (black and gray bars; t test, $p > 0.05$) for both pursuit directions.

Next, we considered how the amplitude and width of the tuning functions were affected by pursuit. For this analysis, we calculated ratios of the parameters for each

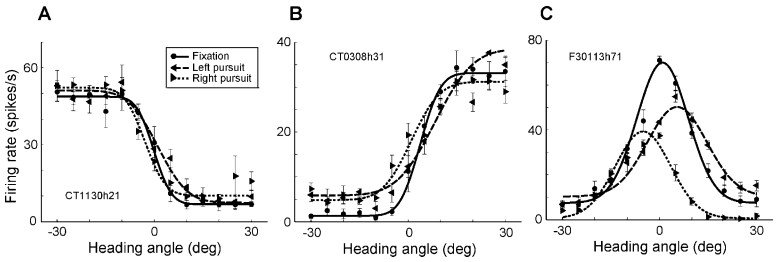

Figure 6. Influence of Pursuit: Example Cells

For each cell, the tuning functions were measured under three different pursuit conditions (no pursuit, solid curves; left pursuit, dashed curves; right pursuit, dotted curves). The tuning functions are plotted in screen coordinates (equivalent to head-centered or egocentric coordinates under our conditions). In all cases, the changes of the neuronal tuning functions were relatively modest.

cell between the pursuit and fixation conditions. The distributions of these ratios are shown in Figures 7B and 7C. The means of these distributions center near unity, suggesting invariance, on average, under pursuit.

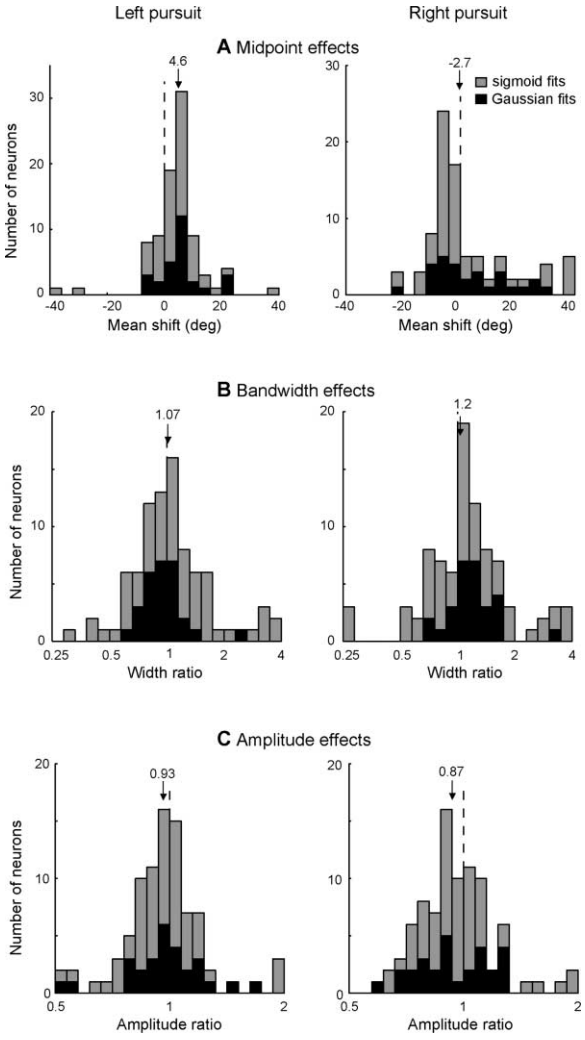

Figure 7. Summary of Pursuit Effects on Tuning Parameters

For each pursuit condition (left, right) and each tuning curve parameter, we show the sample distributions of the magnitude of change in the parameter.

(A) Effects on the center of tuning. This is the difference between the mean of the best-fit functions with and without pursuit.

(B and C) Effects on bandwidth (B) (see Experimental Procedures for definition). For (B) and for the amplitude effects illustrated in (C), we calculated the ratio between the value of the parameter with and without pursuit.

While individual cells were often substantially affected, approximately equal numbers of cells showed increases and decreases, both with respect to amplitude and width. For neither parameter, and for neither direction of pursuit, was there a systematic or statistically significant effect of pursuit for the entire sample of VIP cells (t tests, $p > 0.05$). However, in considering the separate types of tuning, we discovered that the band-pass cells did show a slight increase in tuning width under right pursuit, but this was a modest effect (average ratio $= 1.34$, $p < 0.05$ by paired t test). While this might suggest that band-pass cells become slightly less reliable under pursuit, compared to sigmoidally tuned cells, it is also possible that this apparent difference might disappear with a larger sample.

We also wished to consider whether any of the changes we observed under pursuit might result from additive effects of explicit signals related to pursuit. Such signals could come in two forms. First, one might expect extraretinal eye velocity signals, such as those that have been seen in area MST and VIP (Newsome et al., 1988; Komatsu and Wurtz, 1988; Schlack et al., 2003). Second, because the room is dimly lit by the display and many VIP RFs extend beyond the dimensions of the screen, one might expect visual responses to the pursuit-induced motion of visual contours under pursuit. To evaluate this, we recorded 59 neurons' firing rate during pursuit in the absence of a heading stimulus. Of these 59 cells, only a minority (27% for left pursuit, 41% for right) showed activity that was significantly different during pursuit, compared with fixation. Furthermore, these responses were small and inconsistent in sign. On average, the change in activity was only 17% of the magnitude of the heading stimulus-evoked activity, and for the whole sample was not significantly different from 0 (t test, $p > 0.05$). We cannot tell under our conditions, where the room was not completely dark, whether this activity was visual or extraretinal in source, but for the present purposes it is not important. Overall, then, the responses under pursuit cannot result from a superposition of heading responses and direct pursuit responses, because the direct effects of pursuit were inadequate in magnitude to produce the effects seen in VIP cell's heading tuning. Lastly, superposition of extraretinal signals could not lead to horizontal shifts of the heading tuning functions, which was the dominant result in our data.

Discussion

This study produced two principal results. First, tuning for heading in VIP is robust, with the majority of cells

showing high-amplitude and selective responses to horizontally varying headings. Second, this tuning is remarkably stable in the face of horizontal smooth pursuit eye movements that greatly distort the retinal motion pattern. Thus, the representation of heading in VIP is very nearly in head-centered coordinates, instead of the eye-centered coordinates in which early and intermediate motion representations are found. We will now compare these results with those found in other high-level motion areas and relate them to the psychophysics of heading.

Optic flow has previously been most studied in the medial superior temporal area, MST. This area has large receptive fields that are sensitive to complex motion patterns (Tanaka et al., 1986; Duffy and Wurtz, 1991a, 1991b; Graziano et al., 1994). MST also responds well and directionally to stimuli simulating self-motion (Paolini et al., 2000; Page and Duffy, 1999, 2003) and thus clearly also possesses an accurate representation of heading. However, despite their similarity in these respects, VIP and MST are very distinct in others. VIP is more multimodal than MST, possessing both somatosensory and auditory responses. In addition, the presence of depth-dependent visual RFs in VIP has suggested a role in estimating the motion of nearby objects (Colby et al., 1993). Both the present work and previous studies (Bremmer et al., 2002a) show that the quality of self-motion signals in VIP is very good, and at face value comparable to that in MST (Duffy and Wurtz, 1995; Bradley et al., 1996).

Pursuit compensation, however, seems far more complete in VIP than previous reports indicate is the case in MST. While some MST neurons compensate well for pursuit, thus representing heading in nearly head-centered coordinates, these are a minority. The majority of cells compensate rather little, so that the modal value is not far from retinal coordinates (Bradley et al., 1996; Shenoy et al., 1999, 2002). In addition, many cells show dramatic gain changes under pursuit (Shenoy et al., 1999). However, it is worth emphasizing the difference between these studies and the present one. In the MST experiments, the heading stimulus contained no simulated depth, which provides the distinct advantage that a "simulated eye movement" condition can be used to eliminate extraretinal cues and thus compare visual and extraretinal sources of compensatory signals. The design also allows the direct estimation of the compensation in percent, something that our more natural stimulus design does not allow. Motion parallax cues substantially assist in the perceptual compensation for pursuit eye movements and can even completely support compensation when pursuit speed is low (1–2°/s; Warren and Hannon, 1990). There is some evidence that the addition of parallax cues to depth can substantially influence MST responsiveness (Upadhyay et al., 2000). However, their stimuli were intentionally held fixed in retinal coordinates. Therefore, the finding that tuning was largely unchanged under pursuit might again indicate that the representation in MST is largely in retinal coordinates, even when motion parallax cues to depth are incorporated. While we believe that the results in MST appear quite different, it remains entirely possible that all the apparent differences might be due to the different stimuli used in the MST experiments. Quantitative comparison will have to wait until the same stimuli are used in both structures.

The representation of heading we observe in VIP is very suitable to support observed psychophysical performance for a wide range of forward headings. Not only does the population response seem quite tolerant of pursuit, but the precision of the representation seems very adequate to support perceptual accuracy. The average bandwidth of single neurons in VIP was approximately 5°, and the average response amplitude was approximately 20 spikes/s. If we assume that the variance of individual cell signals is equal to their mean firing rate, then the typical VIP neuron would have the ability to discriminate 2° differences in heading with an accuracy of about 75% correct; this figure is quite similar to the discrimination performance of monkeys (Britten and van Wezel, 2002). By contrast, to achieve this level of performance, Ben Hamed et al. (2003) needed to use a population of about 150 MST neurons. While our sensitivity estimate, which is based on using the steepest point on a tuning function, probably overestimates the actual precision of single cells, it does not take into account improvements that might be gained by using the entire population (e.g., by vector averaging). The sensitivity of the population is likely to be limited by shared noise (Shadlen et al., 1996; Georgopoulos et al., 1986), for which we have no estimate. Nonetheless, it seems clear that VIP contains a representation sufficient to account for perceptual sensitivity.

The existence of signals sufficient to support heading perception does not lead us to conclude that VIP is "the heading area," since the same signals might be useful for a wide variety of tasks. Indeed, many of the cells with the best tuning for heading derived this sensitivity from their horizontal direction selectivity (data not shown). Activity in VIP has been shown to be correlated with performance on a motion-detection task, where the stimuli were tailored to the directional preferences of the neurons being recorded (Cook and Maunsell, 2002). It seems likely to us that VIP would also be involved in object-motion tasks (Colby et al., 1993) and others as well. Most motion tasks require some kind of compensation for eye movements, so this feature also might prove very generally useful to motion perception.

These observations provide some clues as to the underlying mechanisms of heading perception. Numerous models of heading perception have been proposed, using a wide variety of mechanisms. Many of these fall into the category of "template" models, where individual neurons will match a particular heading (Perrone and Stone, 1994, 1998; Zhang et al., 1993). These models are intuitively reasonable and easy to read out: the most active template at any instant indicates the current heading. Unfortunately, our data argue against this category of models, although not strongly enough at present to completely exclude them. The population in VIP contains only a minority of band-pass neurons; these are most consistent with the predictions of template models of heading perception. What is problematic for the models is that this category of cells is both less stable in the face of pursuit and somewhat less sensitive to small heading differences. If these were the cells upon which perception depended, one would expect them to be the most isomorphic with the properties of perception.

Another family of models, however, seems at face value more consistent with the present results. Lappe and Rauschecker (Lappe and Rauschecker, 1994; Lappe and Duffy, 1999) propose a family of sigmoid "basis functions" for heading, which accurately represent heading through a population-code readout rule. These sigmoid functions are not unlike the ones we observe in VIP, as well as what has been observed in MST (Ben Hamed et al., 2003). At present, then, the data do not allow us to firmly exclude one family of models, though we find the basis-function formulation generally more consistent with our results. But in any case, the stability of the representation against pursuit simplifies the readout of the population.

One of the most interesting aspects of our data is the compensation for ongoing pursuit eye movements. This compensation can be done in either of two distinct ways: by direct calculation from the pattern of retinal image motion or by using extraretinal signals of eye velocity. Our results do not allow us to conclude which mechanism is responsible, but it should be possible to address this experimentally. One obvious approach would be to systematically perturb the amount of depth in the scene and look for the effects on tuning. Such an experiment has been performed in area MST (Upadhyay et al., 2000) but the results are not directly comparable, since the optic flow stimuli in that paper varied around a circle.

Previous evidence has indicated, however, that MST is directly involved in the perception of heading, since electrical microstimulation of columns of MST neurons can substantially bias heading judgments (Britten and van Wezel, 1998, 2002). Preliminary data suggest that the same thing is true in VIP, as similar biases were observed when this approach was applied there (T. Zhang and K.H. Britten, 2003, Soc. Neurosci., abstract). Therefore, it seems likely that perception of heading is a distributed cortical function that depends on signals in multiple areas. Very likely the network of areas will extend well beyond VIP and MST, as optic flow signals are present in a number of other areas as well (area 7a: Phinney and Siegel, 2000; Merchant et al., 2003; area PEc: Raffi et al., 2002). There appear to be quantitative differences in the exact nature of the signals present in different areas, which does not argue against their being used simultaneously in perception. However, if this is true, it poses a considerable experimental challenge to more precisely characterize the similarities and differences between the multiple sources of information in use across wide regions of cortex. The next generation of experiments will probably require multiple simultaneous interventions or measurements to more precisely define the manner in which multiple areas contribute to complex perceptions. More immediately, however, it will be important to quantitatively compare the nature of the signals in multiple areas such as MST and VIP, preferably under the same experimental conditions. This will allow the formulation of more specific models of how information can be shared between multiple cortical areas in the performance of complex tasks.

Experimental Procedures

Subjects, Surgery, and Training

Two female rhesus macaques (*Macaca mulatta*) were used in this study. Each was implanted with a head restraint post and a scleral search coil, as described in detail elsewhere (Judge et al., 1980). Prior to recording, each monkey was implanted with a chronic recording cylinder (Crist Instruments) over the intraparietal sulcus (IPS), angled either 30° or 45° posterior to vertical, allowing dorsal-posterior access to VIP. Prior to quantitative data collection, each cylinder was extensively mapped using both physiological and anatomical landmarks to localize area VIP. Monkeys were trained using operant conditioning techniques with juice reward for successfully completed trials. Monkeys were trained to fixate, to make memory-guided saccades to eccentric targets, and to discriminate horizontally varying headings. All animal procedures were approved by the UC Davis Animal Care and Use Committee and fully conformed to ILAR and USDA guidelines for the care and treatment of experimental animals.

Visual Stimuli

Visual stimuli were generated by custom software on a personal computer and displayed on a CRT monitor, which subtended 72° horizontally and 56° vertically at 28 cm viewing distance.

We used simulated 3D optic flow stimuli to investigate the heading tuning properties of VIP neurons. The heading stimulus simulated the self-motion of the monkey toward a 3-dimensional cube of points; a front view is shown in Figure 1A. The center of expansion (absent eye movements, see below) indicates the heading and varied horizontally (−30° to 30°). While heading can in principle also vary vertically, we did not sample this dimension because of the prohibitive number of trials that would have been required. Dots were black (0.1 cd/m^2 luminance) on a gray background (30 cd/m^2). A top view is shown to scale in Figure 1B, illustrating the depth relationships and the relative velocity of the trajectory. The simulated trajectory corresponded to an approach of 1 m/s toward a cloud of points 10 min across. (There is a family of retinally equivalent situations differing only by a scale factor, where observer speed and the size of the dot cloud vary together.)

Cell Recording

The monkeys were seated in a primate chair with their heads restrained. Eye movements were tracked with a scleral search coil system (David Northmore, Inc.) and passed to the experimental control computer.

Preliminary mapping experiments were performed before the single unit recording experiments. The intraparietal sulcus was identified by its appropriate depth and by the presence of adjacent areas with the properties of LIP and VIP, with the putative LIP located dorsal and lateral to VIP. LIP was identified by the presence of numerous cells that showed directional delay or perisaccadic activity on a memory-guided saccade task. VIP was identified based on a high percentage of direction-selective units and its position close to the bottom of IPS. While our monkeys were not trained on a reaching task, we were able to also identify MIP based on activity related to the spontaneous arm movements of the monkeys in the chair. These recording locations were always dorsal, medial, and contiguous with the identified location of VIP. Relative position of VIP in intraparietal sulcus and the mapping results from left hemisphere of monkey F are shown in Supplemental Figure S1 (http://www.neuron.org/cgi/content/full/42/6/993/DC1). Once we were confident of the map, quantitative data collection commenced.

After a single VIP unit had been isolated using standard extracellular techniques, neuronal activity was recorded using tungsten microelectrodes (Fred Haer Co.) introduced through stainless steel guide tube held in place by a plastic grid attached to the inside of the recording cylinder (Crist et al., 1988). We used the public domain software package REX (Hays et al., 1982) to record the time of stimulus events and action potentials with 1 ms resolution.

RF location and size were determined using handheld moving bar stimuli and computer-generated moving dot patches. Then we placed the center of visual stimuli over the most sensitive region of the RF by adjusting the monkey's fixation location. For the random dot stimuli, the size of patches was adjusted to be slightly smaller than the size of the RF. The heading measurements that are the focus of this paper came from blocks of trials containing four types of randomly interleaved trials: fixation trials, two pursuit directions (10°/s), and additional pursuit-only trials where no visual stimulus

was present. A schematic representation of trial timing is shown in Figure 1C. Each trial began with the appearance of the fixation point. After the monkey fixated on it, the stationary stimulus dots would appear; 250 ms later, the fixation point began moving (if the trial included pursuit). Another 250 ms later, the stimulus dots moved for 1 s, then both fixation point and stimulus dots disappeared and the monkey received a juice reward. Typically, a block of trials included 5 trials on each condition, and repeat blocks were collected if time allowed.

Data Analysis

We measured the neuronal responses to our heading stimulus during both fixation and smooth pursuit eye movement. Responses consisted of the total spike count during the 1 s simulated movement period. The 13 data points for each condition were then fit by 2 different functions. A probit function (cumulative Gaussian) of the form

$$R = A \times \left(\frac{1}{\sigma\sqrt{2\pi}} \int_{-\infty}^{h} e^{\frac{-(x-\mu)^2}{2\sigma^2}} dx \right) + b \quad (1)$$

was used, where R is neuronal response, x denotes the heading angle, μ the mean, σ the width, and b the baseline. We also fit each set of data with Gaussian functions of the form

$$R = A \times e^{\frac{-(x-\mu)^2}{2\sigma^2}} + b \quad (2)$$

using the same parameters. The goodness of fit for each was compared (nested likelihood ratio test) to the goodness of fit of the mean alone, and one cell for which neither function described the data significantly better ($p < 0.05$) was discarded from further analysis.

The probit and Gaussian functions both use the parameter σ to represent the breadth of the tuning function, but this parameter has a somewhat different meaning in each function. We sought a measure of bandwidth that would be directly comparable for both classes of cells, and we chose to equate the two in terms of how much heading angle change was required to cause the cells' responses to change by a comparable amount. For all cells, the point of maximum sensitivity is the steepest part of the function (at the mean for the probit functions and at the σ point for the Gaussian). Our derived measure of bandwidth, which we use henceforth, corresponds to the range of heading around this point required for the cell's discharge to change by 25% of its total dynamic range. This corresponded to 0.637σ for cells that were better fit by probit functions and 0.418σ for the cells better fit by Gaussian functions.

Acknowledgments

The authors thank H.R. Engelhardt for animal care and training and A.L. Jones for custom software. We appreciate useful discussions with C.H. McCool, J.B. Maciokas, and H.R Engelhardt, as well as feedback from seminar audiences. Research supported by the Human Frontier Science Program Organization and the National Institutes of Health (EY10562 to K.H.B. and Vision Core Center grant EY12576).

Received: January 28, 2004
Revised: April 19, 2004
Accepted: June 4, 2004
Published: June 23, 2004

References

Andersen, R.A., Shenoy, K.V., Crowell, J.A., and Bradley, D.C. (2000). Neural mechanisms for self-motion perception in area MST. Int. Rev. Neurobiol. *44*, 219–233.

Banks, M.S., Ehrlich, S.M., Backus, B.T., and Crowell, J.A. (1996). Estimating heading during real and simulated eye movements. Vision Res. *36*, 431–443.

Ben Hamed, S.B., Page, W., Duffy, C., and Pouget, A. (2003). MSTd neuronal basis functions for the population encoding of heading direction. J. Neurophysiol. *90*, 549–558.

Blatt, G.J., Andersen, R.A., and Stoner, G.R. (1990). Visual receptive field organization and cortico-cortical connections of the lateral intraparietal area (area LIP) in the macaque. J. Comp. Neurol. *299*, 421–445.

Bradley, D.C., Maxwell, M., Andersen, R.A., Banks, M.S., and Shenoy, K.V. (1996). Mechanisms of heading perception in primate visual cortex. Science *273*, 1544–1547.

Bremmer, F., Duhamel, J.R., Ben Hamed, S., and Graf, W. (2002a). Heading encoding in the macaque ventral intraparietal area (VIP). Eur. J. Neurosci. *16*, 1554–1568.

Bremmer, F., Klam, F., Duhamel, J.R., Ben Hamed, S., and Graf, W. (2002b). Visual-vestibular interactive responses in the macaque ventral intraparietal area (VIP). Eur. J. Neurosci. *16*, 1569–1586.

Britten, K.H., and van Wezel, R.J. (1998). Electrical microstimulation of cortical area MST biases heading perception in monkeys. Nat. Neurosci. *1*, 59–63.

Britten, K.H., and Van Wezel, R.J. (2002). Area MST and heading perception in macaque monkeys. Cereb. Cortex *12*, 692–701.

Colby, C.L., Duhamel, J.R., and Goldberg, M.E. (1993). Ventral intraparietal area of the macaque: anatomic location and visual response properties. J. Neurophysiol. *69*, 902–914.

Cook, E.P., and Maunsell, J.H. (2002). Dynamics of neuronal responses in macaque MT and VIP during motion detection. Nat. Neurosci. *5*, 985–994.

Cooke, D.F., Taylor, C.S., Moore, T., and Graziano, M.S. (2003). Complex movements evoked by microstimulation of the ventral intraparietal area. Proc. Natl. Acad. Sci. USA *100*, 6163–6168.

Crist, C.F., Yamasaki, D.S., Komatsu, H., and Wurtz, R.H. (1988). A grid system and a microsyringe for single cell recording. J. Neurosci. Methods *26*, 117–122.

Crowell, J.A., and Banks, M.S. (1993). Perceiving heading with different retinal regions and types of optic flow. Percept. Psychophys. *53*, 325–337.

Duffy, C.J., and Wurtz, R.H. (1991a). Sensitivity of MST neurons to optic flow stimuli. I. A continuum of response selectivity to large-field stimuli. J. Neurophysiol. *65*, 1329–1345.

Duffy, C.J., and Wurtz, R.H. (1991b). Sensitivity of MST neurons to optic flow stimuli. II. Mechanisms of response selectivity revealed by small-field stimuli. J. Neurophysiol. *65*, 1346–1359.

Duffy, C.J., and Wurtz, R.H. (1995). Response of monkey MST neurons to optic flow stimuli with shifted centers of motion. J. Neurosci. *15*, 5192–5208.

Duhamel, J.R., Bremmer, F., BenHamed, S., and Graf, W. (1997). Spatial invariance of visual receptive fields in parietal cortex neurons. Nature *389*, 845–848.

Duhamel, J.R., Colby, C.L., and Goldberg, M.E. (1998). Ventral intraparietal area of the macaque: congruent visual and somatic response properties. J. Neurophysiol. *79*, 126–136.

Georgopoulos, A., Schartz, A., and Kettner, R. (1986). Neuronal population coding of movement direction. Science *233*, 1416–1419.

Gibson, J.J. (1950). Perception of the Visual World (Boston: Houghton-Mifflin).

Graziano, M.S., Andersen, R.A., and Snowden, R.J. (1994). Tuning of MST neurons to spiral motions. J. Neurosci. *14*, 54–67.

Hays, A.V., Richmond, B.J., and Optican, L.M. (1982). A UNIX-based multiple process system for real-time data acquisition and control. WESCON Conf Proc *2*, 1–10.

Judge, S.J., Richmond, B.J., and Chu, F.C. (1980). Implantation of magnetic search coils for measurement of eye position: an improved method. Vision Res. *20*, 535–538.

Komatsu, H., and Wurtz, R. (1988). Relation of cortical areas MT and MST to pursuit eye movements. I. Localization and visual properties of neurons. J. Neurophysiol. *60*, 580–603.

Lappe, M., and Duffy, C.J. (1999). Optic flow illusion and single neuron behaviour reconciled by a population model. Eur. J. Neurosci. *11*, 2323–2331.

Lappe, M., and Rauschecker, J.P. (1994). Heading detection from optic flow. Nature *369*, 712–713.

Lewis, J.W., and Van Essen, D.C. (2000). Corticocortical connections

of visual, sensorimotor, and multimodal processing areas in the parietal lobe of the macaque monkey. J. Comp. Neurol. *428*, 112–137.

Maunsell, J.H., and van Essen, D.C. (1983). The connections of the middle temporal visual area (MT) and their relationship to a cortical hierarchy in the macaque monkey. J. Neurosci. *3*, 2563–2586.

Merchant, H., Battaglia-Mayer, A., and Georgopoulos, A.P. (2003). Functional organization of parietal neuronal responses to optic-flow stimuli. J. Neurophysiol. *90*, 675–682.

Newsome, W.T., Wurtz, R.H., and Komatsu, H. (1988). Relation of cortical areas MT and MST to pursuit eye movements. II. Differentiation of retinal from extraretinal inputs. J. Neurophysiol. *60*, 604–620.

Page, W.K., and Duffy, C.J. (1999). MST neuronal responses to heading direction during pursuit eye movements. J. Neurophysiol. *81*, 596–610.

Page, W.K., and Duffy, C.J. (2003). Heading representation in MST: sensory interactions and population encoding. J. Neurophysiol. *89*, 1994–2013.

Paolini, M., Distler, C., Bremmer, F., Lappe, M., and Hoffmann, K.P. (2000). Responses to continuously changing optic flow in area MST. J. Neurophysiol. *84*, 730–743.

Perrone, J.A., and Stone, L.S. (1994). A model of self-motion estimation within primate extrastriate visual cortex. Vision Res. *34*, 2917–2938.

Perrone, J.A., and Stone, L.S. (1998). Emulating the visual receptive-field properties of MST neurons with a template model of heading estimation. J. Neurosci. *18*, 5958–5975.

Phinney, R.E., and Siegel, R.M. (2000). Speed selectivity for optic flow in area 7a of the behaving macaque. Cereb. Cortex *10*, 413–421.

Raffi, M., Squatrito, S., and Maioli, M.G. (2002). Neuronal responses to optic flow in the monkey parietal area PEc. Cereb. Cortex *12*, 639–646.

Royden, C.S., Banks, M.S., and Crowell, J.A. (1992). The perception of heading during eye movements. Nature *360*, 583–585.

Royden, C.S., Crowell, J.A., and Banks, M.S. (1994). Estimating heading during eye movements. Vision Res. *34*, 3197–3214.

Saito, H., Yukie, M., Tanaka, K., Hikosaka, K., Fukada, Y., and Iwai, E. (1986). Integration of direction signals of image motion in the superior temporal sulcus of the macaque monkey. J. Neurosci. *6*, 145–157.

Schaafsma, S.J., and Duysens, J. (1996). Neurons in the ventral intraparietal area of awake macaque monkey closely resemble neurons in the dorsal part of the medial superior temporal area in their responses to optic flow patterns. J. Neurophysiol. *76*, 4056–4068.

Schlack, A., Hoffman, K.P., and Bremmer, F. (2003). Selectivity of macaque ventral intraparietal area (area VIP) for smooth pursuit eye movements. J. Physiol. *551*, 551–561.

Shadlen, M.N., Britten, K.H., Newsome, W.T., and Movshon, J.A. (1996). A computational analysis of the relationship between neuronal and behavioral responses to visual motion. J. Neurosci. *16*, 1486–1510.

Shenoy, K.V., Bradley, D.C., and Andersen, R.A. (1999). Influence of gaze rotation on the visual response of primate MSTd neurons. J. Neurophysiol. *81*, 2764–2786.

Shenoy, K.V., Crowell, J.C., and Andersen, R.A. (2002). Pursuit speed compensation in cortical area MSTd. J. Neurophysiol. *88*, 2630–2647.

Tanaka, K., Hikosaka, K., Saito, H., Yukie, M., Fukada, Y., and Iwai, E. (1986). Analysis of local and wide-field movements in the superior temporal visual areas of the macaque monkey. J. Neurosci. *6*, 134–144.

Tanaka, K., Fukada, Y., and Saito, H.A. (1989). Underlying mechanisms of the response specificity of expansion/contraction and rotation cells in the dorsal part of the medial superior temporal area of the macaque monkey. J. Neurophysiol. *62*, 642–656.

Upadhyay, U.D., Page, W.K., and Duffy, C.J. (2000). MST responses to pursuit across optic flow with motion parallax. J. Neurophysiol. *84*, 818–826.

Warren, W.H., Jr., and Hannon, D.J. (1990). Eye movements and optical flow. J. Opt. Soc. Am. A *7*, 160–169.

Warren, W.H., Jr., Morris, M.W., and Kalish, M. (1988). Perception of translational heading from optical flow. J. Exp. Psychol. Hum. Percept. Perform. *14*, 646–660.

Zhang, K., Sereno, M.E., and Sereno, M.I. (1993). Emergence of position-independent detectors of sense of rotation and dilation with hebbian learning: an analysis. Neural Comput. *5*, 597–612.